European Journal of Pharmaceutics and Biopharmaceutics 76 (2010) 159–169

Contents lists available at ScienceDirect

European Journal of Pharmaceutics and Biopharmaceutics

journal homepage: www.elsevier.com/locate/ejpb

Research paper

Microemulsions for oral delivery of insulin: Design, development and evaluation in streptozotocin induced diabetic rats

G. Sharma [a], K. Wilson [a], C.F. van der Walle [a], N. Sattar [b], J.R. Petrie [b], M.N.V. Ravi Kumar [a,*]

[a] Strathclyde Institute of Pharmacy and Biomedical Sciences, University of Strathclyde, Glasgow, UK
[b] BHF Cardiovascular Research Centre, University of Glasgow, Glasgow, UK

ARTICLE INFO

Article history:
Received 29 January 2010
Accepted in revised form 5 July 2010
Available online 22 July 2010

Keywords:
Bioavailability
Insulin
Microemulsions
Oral delivery
Pharmacokinetics
Reverse micelles

ABSTRACT

Insulin loaded microemulsions were developed adopting a low shear reverse micellar approach using didoceyldimethylammonium bromide (DMAB) as the surfactant, propylene glycol (PG) as the co-surfactant, triacetin (TA) as the oil phase and insulin solution as the aqueous phase. A ternary phase diagram was constructed based on multiple cloud point titration to highlight the reverse micellar region. The droplet sizes of the microemulsions were 161.7 ± 24.7 nm with PDI of 0.447 ± 0.076 and insulin entrapment of ~85%. Transmission electron microscopy (TEM) revealed the spherical nature and size homogeneity of the microemulsion droplets. The conformational stability of the entrapped insulin within microemulsions was confirmed by fluorescence spectroscopy and circular dichroism. The microemulsions displayed a 10-fold enhancement in bioavailability compared with plain insulin solution administered *per oral* in healthy rats. The short-term *in vivo* efficacy in STZ induced diabetic rats provided the proof of concept by a modest glucose reduction at a dose of 20 IU/kg. Together this preliminary data indicate the promise of microemulsions for oral delivery of insulin.

1. Introduction

Since the discovery of insulin in the early 1920s [1], millions of people with types 1 and 2 diabetes worldwide have used daily subcutaneous injections to control blood glucose and/or prevent life-threatening ketoacidosis. However, while these injections prolong life and prevent complications, they cause discomfort and inconvenience (leading to problems with adherence to prescribed therapy) and even lipohypertrophy (leading to unpredictable absorption) [2]. Thus, oral delivery of insulin represents an exciting challenge for drug delivery scientists [3], particularly with the prospect of delivering the hormone more physiologically to the liver (via the portal circulation), replicating the dynamics of endogenous release, rather than creating universally high supraphysiological peripheral concentrations as with the parenteral route. However, when administered orally, insulin undergoes severe enzymatic degradation by gastric proteases [4] and undergoes first pass metabolism in the liver [5]. Its high molecular weight renders it impermeable across gastric mucosa, limiting its overall bioavailability and pharmacological action.

Attempts have been made to deliver insulin orally without compromising its stability and pharmacological action. The hexyl-insulin monoconjugate was prepared to protect insulin from gastric proteases and showed a dose dependent glucose-lowering effect in type 1 diabetes patients [6], but detailed pharmacokinetic studies are needed. Incorporation of protease inhibitors were thought to be an option [7], but the side effects such as systemic intoxication and disturbed digestion of food proteins are limitations of this strategy. Complexation with cyclodextrins enhances insulin stability [8], and permeation enhancers (e.g. bile salts and surfactants) improve oral absorption [9], but their toxicity to intestinal mucosa limits the development of clinically viable formulations.

The last few decades have seen overwhelming activity in protein and peptide drug delivery via the oral route, utilizing hydrogels [10], liposomes [11], microparticles [12] and nanoparticles [13]. Controlled release colloidal drug carriers like microemulsions that are the ternary systems of surfactant, oil and water [14] and reverse micelles that are surfactant aggregates in an organic liquid, also showed promise in improving oral bioavailability of insulin in animal studies. Microemulsions are stable isotropic transparent colloidal systems composed of surfactant molecules oriented with their hydrophilic head inwards creating an aqueous core and their hydrophobic tails directed towards outside solubilised in organic phase forming the corona [15]. Formation of such systems is spontaneous and usually takes place above the critical micellar concentration (CMC) of the surfactant at which the surfactant forms well defined molecular structures based on the content of aqueous phase, organic phase and the surfactant used. Microemulsions and reverse micelles have long been used for stabilization of

* Corresponding author. Address: Strathclyde Institute of Pharmacy and Biomedical Sciences, University of Strathclyde, 27 Taylor Street, Glasgow G4 0NR, UK. Tel.: +44 141 548 5948.
E-mail address: mnvrkumar@strath.ac.uk (M.N.V. Ravi Kumar).

0939-6411/$ - see front matter © 2010 Elsevier B.V. All rights reserved.
doi:10.1016/j.ejpb.2010.07.002

proteins in organic solvents [16], protein purification [17] and micro-reactors [18]. Their employment in drug delivery [19,20] lies in their inherent thermodynamic stability, protection of drugs against enzymes, ease of preparation, ability to encapsulate a wide spectrum of drugs with diverse physicochemical properties, and compatibility with oral route. The increase in insulin bioavailability via these carriers has been attributed to protection afforded by them against gastric enzymes, their prolonged retention in the gut and their excellent penetration properties across the GI mucosa [21].

The current report discusses the development of insulin loaded microemulsions for oral delivery and evaluation of their glucose-lowering ability in streptozotocin induced diabetic rats.

2. Materials and methods

2.1. Materials

Bovine serum insulin (nominal strength ~27 units/mg) was purchased from Fluka (UK). Didoceyldimethylammonium bromide (DMAB, 98%) and streptozotocin (STZ) were purchased from Aldrich (UK). Propylene glycol (PG), sodium hydroxide and hydrochloric acid were purchased from Fisher Scientific Corporation (UK). Triacetin (TA) was purchased from Acordis Fine Chemicals (UK). Bovine serum insulin specific ELISA kits were purchased from Mercodia (UK). Distilled water was prepared in house and was used for preparing all the solutions and dilutions. All the chemicals were of reagent grade and were used as received.

2.2. Ternary phase diagram construction

The existence of the microemulsion region was identified by preparing various pseudoternary compositions and evaluating the optical clarity of the compositions at 450 nm. Microemulsions are characterized by transparent optically clear properties that are indicative of stable isotropic phase throughout the formulation. These systems are ternary phases where two immiscible phases (water and oil) are present with a surfactant and a co-surfactant. The surfactant molecules may form a monolayer at the interface between the oil and water, with the hydrophobic tails of the surfactant molecules dissolved in the oil phase and the hydrophilic head groups in the aqueous phase. To quantify the optical clarity of an individual system at a number of compositions while minimising the materials and experimental time, a rapid screening approach was adopted. Briefly, varying amounts of surfactant (2:3 w/w DMAB/PG) (S_{mix}) and oil (TA) were micropipetted into a glass flat-bottomed, 96-well microplate (300 μl well capacity, Fisher, UK) and mixed thoroughly. For each phase diagram, oil and S_{mix} were mixed in different volume ratios from 1:9 to 9:1. Seventeen different ratios were screened to investigate increasing concentrations of S_{mix} to oil and oil to S_{mix} (1:9,1:8, 1:7, 1:6, 1:5, 1:4, 1:3, 1:2, 1:1, 2:1, 3:1, 4:1, 5:1, 6:1, 7:1, 8:1 and 9:1). Pseudoternary phase diagrams were constructed using aqueous titration method, where water was added to each well containing oil and S_{mix}, to give an aqueous volume of 5–90% v/v (in 5% intervals) of the total well volume, the water phase contained insulin for insulin loaded microemulsions. The plates were incubated at room temperature on a plate shaker (700–900 rpm) for 10 min, allowing thorough mixing of all components to give a desired ternary composition. Each composition was produced in triplicate. Absorbance readings for all the compositions were obtained at a wavelength of 450 nm using a microplate reader (Ascent Technologies, Alabama, US) to quantify clarity of the systems. The calculation for the addition of aqueous phase was done by calculating the percentage of each component of the emulsion present at each 5% v/v addition. For the purpose of explanation, a 1:9 ratio of oil and S_{mix} was selected, and the aqueous phase was added using a micropipette at around 5% v/v intervals (Table 1) by mixing on a vortex mixer to give a desired pseudoternary composition.

2.3. Visual observation studies

Following analysis of absorbance for different ternary compositions, it was observed that certain regions varied greatly in composition but had similar absorbance ranges. It was believed that further study on these specific compositions may highlight differences in physical state between these ratios. The results from rapid screening technique were then carried forward to identify certain ratios for further characterization. Larger quantities of these ratios were made to visually observe the physical properties against a dark background to assess the level of transparency. After each 5 % (v/v) addition of aqueous phase to oil and S_{mix} mixture, visual observations were made against a dark background, and different phases were identified based on their observed properties; i.e. clear transparent liquid (microemulsion), cloudy liquid, clear transparent gel, white opaque liquid (macroemulsion), white opaque gel and phase separation. Combined together, the absorbance readings for different phase compositions and associated visual observations lead to generation of a ternary phase diagram that was plotted using ProSim ternary diagram application Software (Labege, Cedex, France).

2.4. Formulation selection

From the ternary diagram and visual observations, a precisely defined composition was selected for fabrication of microemulsion. Briefly, S_{mix} was prepared by mixing DMAB and PG (warmed to 100 °C) in the ratio 3:2 (w/w), and the mixture was stirred at 600 rpm at 100 °C till DMAB dissolved completely in PG. Next, TA was added in the S_{mix} to obtain the desired ratio of 3:1 (S_{mix}/TA) and heating was continued for next 5 min after which the contents were brought down to room temperature (25 °C). This was followed by addition of aqueous phase (distilled water) in the S_{mix}–TA mixture while stirring, in a way that final concentration of aqueous phase in the mixture was 20% v/v. The contents were further stirred for 15 min to ensure microemulsion formation that was monitored by checking the optical clarity and physical property of the system. For preparing drug loaded microemulsion, same

Table 1
Calculation of percentage of oil, surfactant and water used in the construction of phase diagram based on rapid screening approach. Oil:S_{mix} (1:9).

Oil (μl)	S_{mix} (μl)	Water (μl)	Total volume (μl)	Oil%	S_{mix}%	Water %
10	90	0	100	10.0	90.0	0.0
10	90	10	110	9.1	81.8	9.1
10	90	20	120	8.3	75.0	16.7
10	90	25	125	8.0	72.0	20.0
10	90	35	135	7.4	66.7	25.9
10	90	45	145	6.9	62.1	31.0
10	90	55	155	6.5	58.1	35.5
10	90	65	165	6.1	54.5	39.4
10	90	85	185	5.4	48.6	45.9
10	90	100	200	5.0	45.0	50.0
10	90	120	220	4.5	40.9	54.5
10	90	150	250	4.0	36.0	60.0
10	90	190	290	3.4	31.0	65.5
5	45	120	170	2.9	26.5	70.6
5	45	150	200	2.5	22.5	75.0
5	45	200	250	2.0	18.0	80.0
2.5	22.5	150	175	1.4	12.9	85.7
2.5	22.5	225	250	1.0	9.0	90.0

protocol was adopted with a single modification where distilled water was replaced by insulin solution as the aqueous phase. Briefly, 1 mg insulin was dissolved in 110 μl 0.05 M sodium hydroxide, and this solution was diluted with distilled water to adjust the final volume required for addition to S_{mix}–TA mixture.

2.5. Microemulsion droplet size analysis

The droplet size and polydispersity index (PDI) was determined using dynamic light scattering technique employing Zetasizer (Nano ZS, Malvern, UK) taking the average of three measurements. Light scattering was monitored using back scattering angle of 173° at 25 °C, with polystyrene beads used as a standard. In this study, a cumulants analysis algorithm was used that fitted a single exponential to the correlation function to obtain mean size (*Z*-average diameter) and an estimate of the width of the distribution (PDI). Both undiluted and diluted formulations were used for the study.

2.6. Entrapment efficiency

The percentage of insulin incorporated in microemulsion was determined by centrifuging the insulin loaded microemulsions and separating the supernatant. The centrifugation step precipitated the droplets that were then broken down using 500 μl of 1 M hydrochloric acid. The system was then stirred for 1 h to ensure complete breakage of micelles; following stirring, the solution was centrifuged at 14,000*g* for 30 min. The waxy layer of precipitated DMAB was discarded and then 100 μl of the remaining liquid was diluted in 4.9 ml of water. This solution was then analysed for insulin content using the spectrofluorimetry method having a linearity range of 1–10 μg/ml and 0.9987 as correlation coefficient. Samples were loaded into a 1 ml glass cuvette, and insulin was excited at 280 nm and emission was monitored between 290 and 390 nm. The excitation and emission slits were set at 5 nm each, and scan rate of 600 nm/min was used with photomultiplier tube detector voltage at 600 V.

2.7. Microemulsion droplet size as a function of the ternary components

To determine the effect of concentration of different formulation excipients on size and PDI of microemulsions, six different sets of experiments were performed where TA, PG and DMAB each in turn were altered with respect to their concentrations from the selected composition without changing the concentration of other components of the formulation. Each of the three components were in turn doubled and then tripled with respect to their original quantity. The change in particle size and PDI was monitored using dynamic light scattering in triplicate as described earlier.

2.8. Effect of insulin loading on droplet size of microemulsion

Microemulsions were prepared by varying the amount of initial insulin loading. Six different loadings of insulin were selected for these studies: 1.1%, 2.2%, 4.4%, 6.6%, 8.8% and 11.1% w/v with respect to final formulation volume of 450 μl. For each group, formulations were prepared in triplicate as described in previous section. For each drug loading, the size and PDI of prepared microemulsions was monitored and analysed to determine whether drug loading had any significant effect on properties of microemulsion formed.

2.9. Effect of dilution on droplet size of microemulsion

Dilution has a significant effect on the physiochemical properties of microemulsion. Accounted for the fact, dilution causes change in the concentration of aqueous phase which in turn disturbs its ratio with oil phase and surfactant, thereby leading to change in properties of such systems. Herein, we investigated the effect of dilution on droplet size and PDI. Microemulsions were prepared as described in previous section with 2.2% w/v insulin loading. Three different volumes of microemulsion, 50, 25 and 5 μl, were diluted in 5 ml of distilled water after which droplet size and PDI analysis were carried out using the dynamic light scattering.

2.10. Fluorescence spectroscopy

Intrinsic fluorescence spectroscopic experiments were carried out to assess any change in the three-dimensional structure (the local environment of aromatic residues) of insulin. Measurements were carried out at 25 °C in 1 cm path length quartz cuvettes using a fluorescence spectrophotometer (Cary Eclipse, Varian Ltd., UK). The excitation wavelength was 280 nm and intrinsic fluorescence emission was measured in the range 290–390 nm. The excitation and emission slits were set at both 5.0 nm and the scan rate was kept at 600 nm/min with photomultiplier tube detector voltage at 600 V. Insulin was recovered from microemulsions by following similar extraction process discussed under Section 2.6. The fluorescence spectrum of extracted insulin was compared with native insulin of same concentration to study any changes in the molecule. An average of three scans was performed for each sample.

2.11. Circular dichroism (CD)

To verify the integrity of the secondary structure of insulin when entrapped in microemulsion, CD studies were carried out. CD spectra were acquired at 25 °C using a Chirascan Spectropolarimeter (Applied Photophysics, Surrey, UK) in the far UV region (190–250 nm) in a 0.01 cm pathlength cell using a step size of 1 nm. The lamp housing purged with nitrogen, and an average of three scans was obtained. Insulin was extracted from the microemulsions using the previously stated protocol (Section 2.6). CD spectra of the appropriate blank reference were recorded and subtracted from the insulin spectra, to eliminate contributions from the aqueous phase. The mean residual molar ellipticity was calculated from the raw CD signal using a mean residue weight of 116 Da and insulin concentration calculated from the corrected absorbance of the insulin solution at 280 nm.

2.12. Transmission electron microscopy (TEM)

The morphology of insulin loaded microemulsions was investigated using TEM (LEO 912, Cambridge, UK). Formvar/Carbon-coated 200 mesh copper grids were glow discharged and specimens in distilled water were dried down to a thin layer onto the hydrophilic support film. Twenty microlitres of 1% aqueous methylamine vanadate (Nanovan; Nanoprobes, Stony Brook, NY, USA) stain was applied, and the mixture dried down immediately with filter paper to remove excess liquid. The dried specimens were imaged with a LEO 912 energy filtering transmission electron microscope at 120 kV. Contrast enhanced, zero-loss energy filtered digital images were recorded with a 14 bit/2 K Proscan CCD camera.

2.13. Pharmacokinetic studies

Pharmacokinetic studies were carried out in healthy male Sprague Dawley (SD) rats weighing between 250 and 300 g with $n = 3$ animals per time point at an insulin dose of 20 IU/kg body weight of the animal. All the rats used in the pharmacokinetic studies had access to food and water *ad libitum*, and no change was made in their natural homeostasis. All animal experiments were performed

according to project licence duly approved by the Home Office (UK). Animals were divided into 6 groups. Groups I, II and III received insulin microemulsions orally using gavage needle, whereas groups IV, V and VI received same dose of insulin solution in phosphate buffer orally. Blood (50 μl) was withdrawn from tail vein and was centrifuged at 10,000*g* for 5 min, and plasma was separated and stored at −20 °C until further analysis. Multiple blood sampling was carried out in groups I and IV at 0.25, 1, 6 and 12 h with final sampling at 24 h after which animals were sacrificed. To generate the pharmacokinetic profile over 3 days, II, III, V and VI groups were incorporated in the study. Blood sampling in groups II and V was carried out at a single time point (48 h from dosing) after which animals were sacrificed. Similarly, blood sampling in groups III and VI was carried out at a single time point (72 h from dosing) after which animals were sacrificed. After sacrificing the animals, their tissues (spleen, kidneys, liver, pancreas and intestine) were collected for organ pharmacokinetic analysis. All tissues were cleaned, removing any blood and connective tissue and were then weighed and to which phosphate buffer saline was added (volume used equals four times the weight of the tissue). Each tissue was then homogenised (Polytron PT 4000, Kinematica) for 2 min at 25,000 rpm after which it was centrifuged at 14,000*g* for 30 min. The pellet obtained was rejected and supernatant was stored at −20 °C until further analysis. Insulin was quantified in blood samples and in tissue homogenates using bovine serum insulin specific ELISA kits (Mercodia, UK). Statistical analysis of the data was performed via unpaired *T*-test using SigmaStat 2.0 software (Jindal Scientific); a value of $p < 0.05$ was considered significant.

2.14. Pharmacodynamic studies in streptozotocin induced diabetes model

Pharmacodynamic studies were carried out in diabetic male Sprague Dawley (SD) rats weighing between 250 and 300 g with $n = 6$ animals per group at an insulin dose of 20 IU/kg body weight of the animal. All animal experiments were performed according to project licence duly approved by the Home Office (UK). Animals were made diabetic by a single intraperitoneal injection of STZ (in 10 mM ice cold citrate buffer, pH 4.5) at a dose of 55 mg/kg body weight of the animals. All rats were allowed to stabilize for 2 days and housed with 12 h dark–light cycle and access to food and water *ad libitum*. Only the rats with plasma glucose levels (PGL) > 2.5 mg/ml were considered diabetic and used in the study. Animals were divided into four groups with group I as the positive control without any treatment, group II received insulin loaded microemulsions orally, group III was administered insulin loaded microemulsions subcutaneously and group IV was administered with plain insulin solution (in phosphate buffer saline) subcutaneously. Blood (50 μl) was withdrawn from tail vein at 2, 6, 12, 24, 48 and on 72 h from all the groups, and PGL were estimated using the Accu-Check Aviva Nano® Glucometer (Roche diagnostics, Germany). Statistical analysis of the data was performed via unpaired *T*-test using SigmaStat 2.0 software (Jindal Scientific); a value of $p < 0.05$ was considered significant.

3. Results and discussion

3.1. Ternary phase diagram

Fig. 1 shows the ternary phase diagram constructed from our rapid screening approach that coincides with ternary systems reported in the literature [22]. This rapid approach allowed fast throughput of 17 ratios with 18 different volumes of aqueous phase. Fig. 2 depicts the ternary phase diagram constructed using the combination of absorbance readings at 450 nm with visually observed physical properties of different ternary compositions. The combined approaches lead to clear isotropic microemulsion (region A in the ternary phase diagram in Fig. 2) with good coverage of total ternary diagram area. No change was found in the

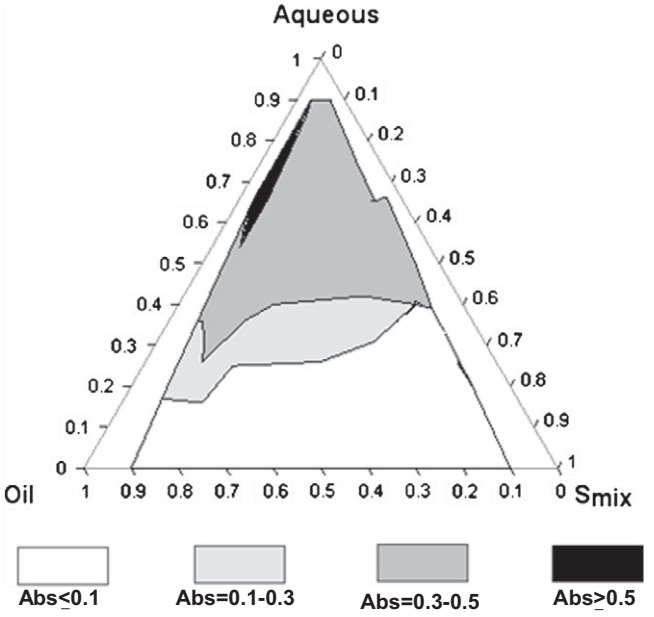

Fig. 1. Ternary diagram constructed using rapid screening procedure using S_{mix} DMAB/PG ratio of 3:2 (w/w)) oil (TA) and water (aqueous phase). Optical clarity was measured at $\lambda = 450$ nm. The key shows the absorbance ranges measured for delineating different regions in the ternary phase diagram.

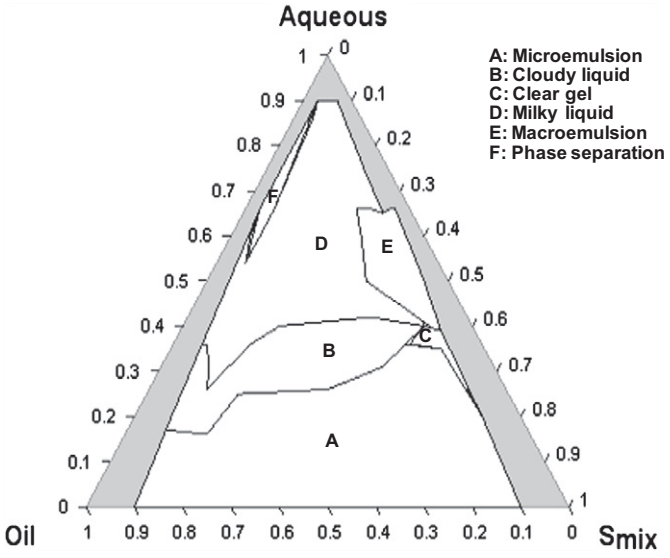

Fig. 2. Different phase obtained in the ternary diagram constructed using rapid screening procedure in combination with visual observations using S_{mix} DMAB/PG ratio of 3:2 (w/w)) oil (TA) and water (aqueous phase). Optical clarity was measured at $\lambda = 450$ nm. The phases were checked for their flow ability and gelling behaviour using the slide tilt method at 45°. A = reverse micellar systems or microemulsion region characterized by clarity and flow ability; B = cloudy liquid, optically unclear with flow properties. This is the region where formation of macroemulsion starts; C = clear gel phase, optically clear but no flow ability, region of swollen reverse micelles; D = milky liquid, highly opaque with flow properties, region of macroemulsion; E = milky gel, swollen macroemulsion with opaqueness and poor flow properties; F = phase separation, region where the whole system breaks down and aqueous and oil layers separate out forming two distinct layers.

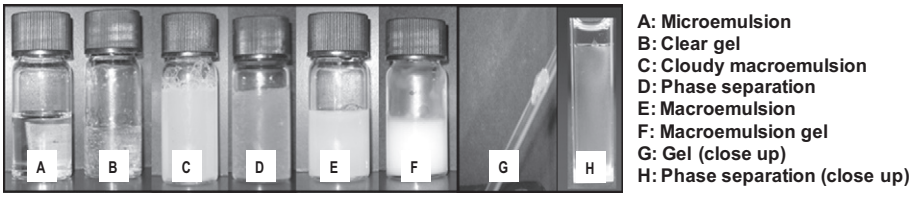

Fig. 3. Visual observation of different phases attained during construction of ternary phase diagram constructed using rapid screening procedure using S_{mix} DMAB/PG ratio of 3:2 (w/w)) oil (TA) and water (aqueous phase). Optical clarity was measured at λ = 450 nm. [A] = S_{mix}/oil 2:1 with aqueous phase making 35% of the total volume (microemulsion). [B] = S_{mix}/oil 9:1 with aqueous phase making 25% of the total volume (clear gel). [C] = S_{mix}/oil 1:7 with aqueous phase making 20% of the total volume (cloudy macroemulsion). [D] = S_{mix}/oil 1:8 with aqueous phase making 75% of the total volume (phase separation). [E] = S_{mix}/oil 1:6 with aqueous phase making 50% of the total volume (macroemulsion). [F] = S_{mix}/oil 8:1with aqueous phase making 35% of the total volume (swollen macroemulsion gel). [G] = Slide inclined at 45° having the formulation showing gel formation. [H] = Phase separation phenomenon as seen more closely using glass cuvette.

phase behaviour of the ternary phase diagram when insulin solution was included in the formulation as the aqueous phase, which may be due to the fact that the formation and stability of microemulsion consisting of combination of non-ionic PG and cationic DMAB surfactants are not affected by the change in pH or ionic strength.

3.2. Visual observations

The ternary compositions were also analysed visually for their physical state since formulations with similar absorbance readings differed markedly in their actual ternary compositions (Fig. 3). Clear isotropic microemulsions were formed when S_{mix}:oil ratio was kept at 2:1 with aqueous phase forming 35% v/v of total composition. When S_{mix}:oil ratio was increased to 9:1 with aqueous phase volume making 25% v/v of total composition, transparent gel formulations were formed, and this may be described due to high surfactant content of the ternary composition that causes hydration and swelling of surfactants resulting in formation of macromolecular gels. On the other hand, when S_{mix}:oil ratio was reduced to 1:7 with aqueous phase making 20% v/v of total composition, cloudy macroemulsions were formed and on further reducing the S_{mix}:oil ratio to 1:6 with aqueous phase making 50% v/v of total composition, milky macroemulsions were formed. This indicated that when S_{mix}:oil ratio was changed from 1:7 to 1:6 with subsequent increase in aqueous phase volume from 20 to 50% v/v, the system underwent destabilization resulting in aggregation of water droplets to form structures like macroemulsions which was evident by development of turbidity (as the droplet size was greater than domains of visible light) that increased on further changing the S_{mix}:oil ratio from 1:7 to 1:6. When S_{mix}:oil ratio was changed from 6:1 to 1:1, more absorbance readings were obtained for clear microemulsion phase, but this was limited to total aqueous phase content below 35%. Hydration and swelling of surfactant molecules was evident when S_{mix}:oil ratio was kept at 8:1 with aqueous phase making 35% v/v of total composition, and this resulted in formation of swollen macroemulsion gels. Complete phase separation was observed when S_{mix}:oil ratio was 1:8 with aqueous phase forming 75% v/v of total composition, and this may be attributed to complete destabilization and aggregation of microemulsion droplets (aqueous phase) due to inability of the S_{mix} to stabilize the relatively large aqueous phase content in large amounts of oil.

3.3. Formulation development and insulin entrapment

The use of microemulsions for protein solubilisation is well reported in the literature, and they have been defined as L-2 phases capable of solubilising 10% (w/w) of water. The emulsions (w/o type) based on reverse micellar approach can be defined by the classical definition given by Danielsson and Lindman [23] where water, oil and surfactant together form thermodynamically stable isotropic clear systems with droplet size in the nanometre range. Herein, we developed DMAB based microemulsions with a low shear process that involved mixing of components in a sequential manner and where a polyol (PG) was used as the co-surfactant and TA was used as the oil phase. Insulin was entrapped inside the reverse micellar systems in the aqueous core. DMAB is a cationic surfactant with HLB values around 18 [24], and this affords considerable lowering of interfacial tension allowing water molecules to be solubilised in the internal core of the micelles; it is also safe and non-toxic at the concentrations used [25]. PG was incorporated as a co-surfactant, increasing interfacial fluidity by penetration into the DMAB film and creating disorder. TA is routinely used in oral pharmaceutical formulations being regarded as a non-toxic, non-irritating, with good biocompatible properties [26], and its solubility in water (1 in 14 parts) makes it ideal oil phase in this study.

Insulin entrapment in microemulsions was evaluated after sedimenting and cracking the micelles using centrifugation and hydrochloric acid, respectively. The extracted insulin was then diluted with distilled water and analysed. The results indicated more than 85% of insulin was entrapped in the system, in agreement with the physicochemical properties of the system. Insulin is soluble in both acidic and alkaline solutions, sparingly soluble in non-buffered water and completely insoluble in hydrophobic oils like TA that makes the environment inside reverse micellar core an ideal place to partition insulin from the oil phase (TA).

3.4. Microemulsion droplet size as a function of the ternary components

Fig. 4 depicts the size distribution intensity curves obtained for blank and insulin loaded microemulsions. The *Z*-average diameter obtained from these size distribution histograms clearly showed that blank formulations had an average droplet size of 104.8 ± 3.05 nm with a PDI of 0.302 ± 0.006, whereas insulin loaded systems had an average droplet size of 161.7 ± 24.7 nm with a PDI 0.447 ± 0.076. The microemulsion state is characterized by a delicate balance between the oil, surfactant and aqueous phase. Any change in the composition can affect the microemulsion structure both in terms of size and physicochemical properties. Fig. 5 shows the effect of DMAB concentration on droplet size of microemulsion. When DMAB concentration was doubled, there was a very large increase in droplet size from 161.7 + 24.7 nm to 24.6 + 2.1 μm, and this effect was more pronounced when the amount of DMAB was tripled compared to the original formulation. Similarly, PDI of formulations displayed an increasing trend with an increase in DMAB concentration. Increase in particle size and PDI of microemulsion droplets with an increase in DMAB concentration can be attributed to the following reasons: (i) increase in the amount of water solubilised with an increase in

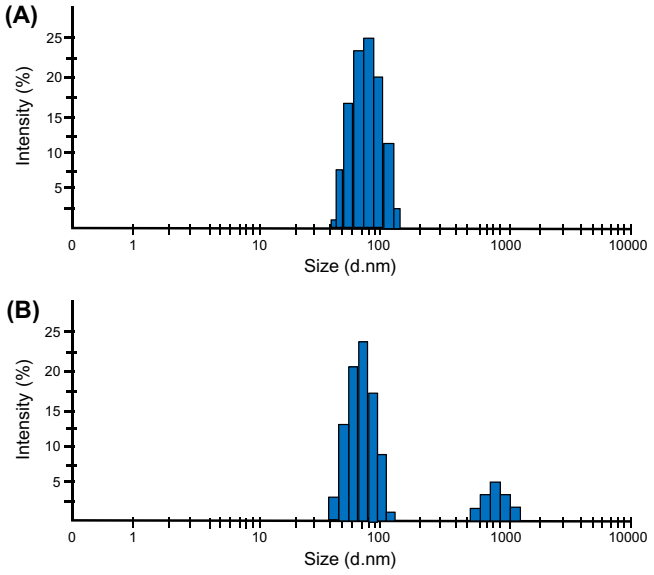

Fig. 4. Size (hydrodynamic diameter) versus % intensity histograms (size distribution) obtained using dynamic light scattering measurements for (A) blank microemulsion and (B) insulin loaded microemulsion with 2.2% drug loading. The results shown are average of three measurements at 25 °C. (For interpretation of the references to colour in this figure legend, the reader is referred to the web version of this article.)

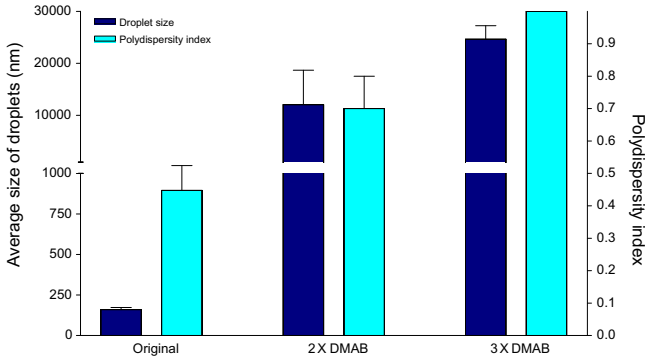

Fig. 5. Effect of DMAB (surfactant) concentration on droplet size and PDI of microemulsions droplets at 25 °C. The original formulations had 2.2% w/v as insulin loading in 0.05 M sodium hydroxide making 20% aqueous phase. Data represents mean with standard deviation at $n = 3$. (For interpretation of the references to colour in this figure legend, the reader is referred to the web version of this article.)

surfactant concentration resulting in formation of bigger emulsion droplets leading to development of heterogeneity in droplet sizes which subsequently causes increase in PDI of microemulsion and (ii) enhanced molecular diffusion of aqueous phase from smaller to larger droplets through continuous oil phase which causes an increase in size of larger droplets at the expense of smaller droplets [27].

Morphological characterization of the droplets was acquired by TEM, to complement the DLS data acquired above. TEM images of the formulations are presented in Fig. 6 which confirmed that droplets were well dispersed without any aggregation or cluster formation, spherical in shape, appreciably homogeneous with submicron sizes. The diameters of the droplets determined by TEM were slightly smaller than determined by DLS, and this can be attributed to the differences in sample preparation: DLS being carried out in the liquid state where the micelles are relatively hydrated/swollen, with TEM involving a drying step that results in micelle dehydration/shrinkage [28].

When the amount of PG was doubled, there was an increase in the droplet size from 161.7 ± 24.7 nm to 1005.8 ± 221.3 nm (Fig. 7). This may be attributed to the fact that the addition of co-surfactant leads to greater penetration of the aqueous phase in the hydrophilic region of the surfactant monomers. On increasing the amount of PG threefold, no change in droplet size was seen, and this may be due to the saturation of voids between DMAB molecules by PG at the interface. It should be noted that the increase in PG was accompanied by changes in the PDI, although the mechanisms for this are unclear.

When the amount of TA was doubled, there was a very large increase in droplet size and PDI (Fig. 8), possibly due to the reduction in overall S_{mix} concentration compared with original composition, such that larger droplets were generated in order to minimise the surface area of the oil–water interface [29]. Interestingly, when the amount of TA was tripled, there was a decrease in droplet size and an increase in PDI, which may be attributed to dilution of a heterogeneous mix of droplet sizes, less likely to coalesce through reduced probability of contact.

3.5. Effect of insulin loading and dilution on microemulsion droplet size

Fig. 9 shows that loading of insulin in the aqueous phase increased the droplet size compared to the blank. This was attributed to the amphiphilic nature of polypeptides such as insulin facilitating its adsorption at the interface within emulsion systems [30]. In this case, insulin adsorption at the interface may partially displace surfactant/co-surfactant, destabilizing the microemulsions and so increasing droplet size. When insulin was loaded from 1.1% to 4.4% w/v into the aqueous core, there was no statistical difference in the size of droplets but above 4.4% w/v insulin loading, droplet size increased significantly. Insulin loading above 4.4% w/v may therefore represent a particular saturation of insulin within the aqueous phase such that partition to the interface or oil phase itself leads to destabilization of the microemulsion system.

For insulin loadings of 4.4% w/v, there was no significant change in droplet size and PDI of microemulsion upon dilution with water (Fig. 10). The mechanism underlying droplet stability during phase inversion is thought to involve initial merger of the water droplets forming a bilamellar continuous phase [31] followed by breakdown into droplets facilitated by the lowest interfacial tension near the inversion point. The high S_{mix} (DMAB + PG) content of our formulation allowed for the complete solubilisation of TA near the inversion point, but to achieve this a large amount of water was required for dilution.

3.6. Conformational integrity of insulin

Insulin contains tyrosine residue positions 14 and 19, which fluoresce upon excitation at 280 nm; the emission maximum and intensity being dependent on the local environment, since water causes a red-shift and quenching of their intrinsic fluorescence [32]. Therefore, fluorescence spectroscopy can be used to monitor changes in the structure of insulin. Fig. 11 shows the fluorescence emission spectra of native insulin compared with fluorescence spectra of insulin extracted from the microemulsion. The small decrease in emission intensity without red-shift is suggestive of a minor change in the local environment of the tyrosine residues, the wavelength of the emission maximum being consistent with previous data for insulin microemulsion [33].

To correlate the small change in the aromatic environment observed above, with possible change in the secondary structure of insulin, we used CD in the far UV region, which corresponds to peptide backbone. Fig. 12 shows the CD spectrum of native insulin compared with CD spectrum of insulin extracted from microemulsions. Both spectra show clear minima of similar magnitude at 209

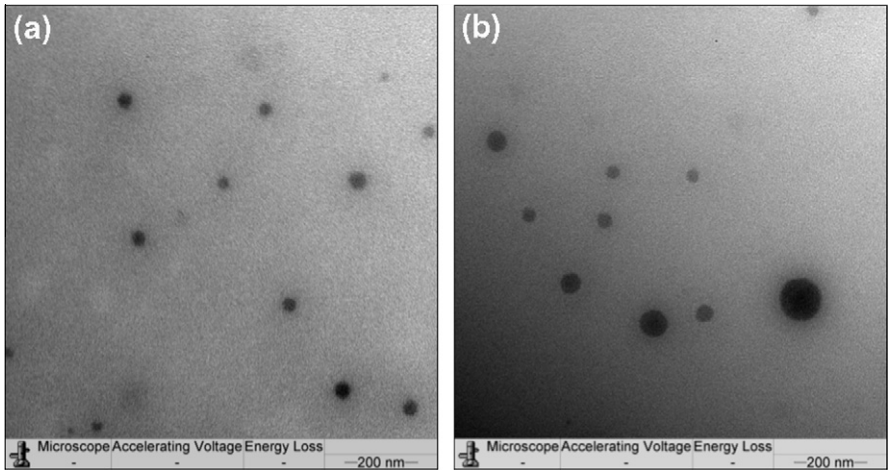

Fig. 6. Transmission electron micrographs of blank microemulsion droplets (a) and insulin loaded microemulsion droplets (b). The micrograph clearly shows the spherical nature of droplets, absence of any aggregation and increased polydispersity in insulin loaded systems. The formulations had 2.2% w/v as insulin loading in 0.05 M sodium hydroxide making 20% aqueous phase. Scale bar 200 nm and magnification 12,500×.

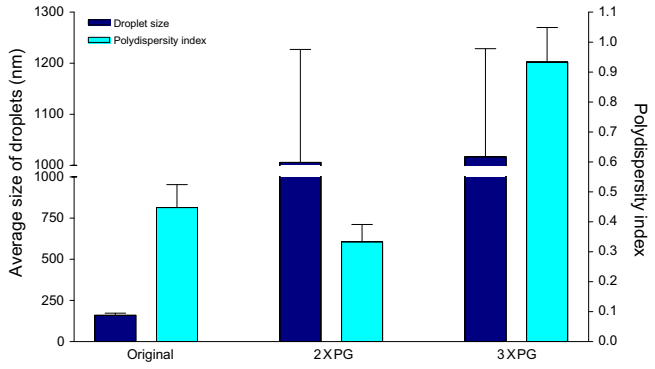

Fig. 7. Effect of PG (co-surfactant) concentration on droplet size and PDI of microemulsion droplets at 25 °C. The original formulations had 2.2% w/v as insulin loading in 0.05 M sodium hydroxide making 20% aqueous phase. Data represents mean with standard deviation at $n = 3$. (For interpretation of the references to colour in this figure legend, the reader is referred to the web version of this article.)

and 222 nm, which are indicative of the known α-helical conformation of insulin [34]. The reduced maxima at 195 nm indicate a relative loss of helical structure for insulin following encapsulation and extraction from the microemulsion system. This suggests that insulin underwent adsorption at the interface within the emulsion system, which is commonly associated with some degree of unfolding [30]. Nevertheless, the close similarity of the fluorescence and CD spectra of the native and extracted insulin samples indicates only minor conformational changes in the secondary and tertiary structure of insulin during the encapsulation process.

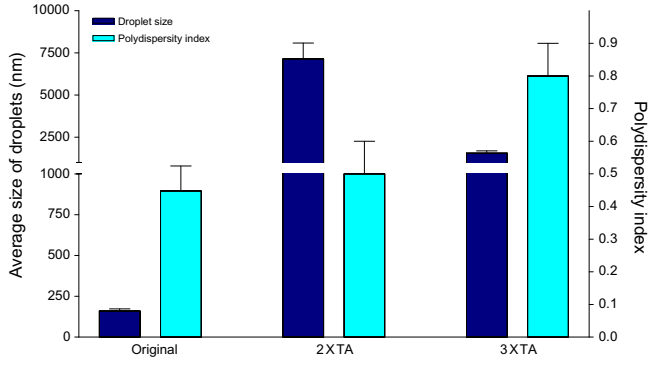

Fig. 8. Effect of TA (oil phase) concentration on droplet size and PDI of microemulsion droplets at 25 °C. The original formulations had 2.2% w/v as insulin loading in 0.05 M sodium hydroxide making 20% aqueous phase. Data represents mean with standard deviation at $n = 3$. (For interpretation of the references to colour in this figure legend, the reader is referred to the web version of this article.)

3.7. Pharmacokinetic studies

Blood levels of insulin after oral administration of microemulsions and plain insulin solution were compared using bovine serum insulin specific ELISA kits. Fig. 13 depicts the plasma concentration versus time profile of insulin obtained from the microemulsions compared with plain insulin solution in phosphate buffer saline, administered orally. The microemulsions demonstrated a higher C_{max} (18.4 ± 2.6 μIU/ml) and a longer T_{max} (6 h) compared with plain insulin solution ($C_{max} \sim 1.84 \pm 0.1$ μIU/ml and $T_{max} \sim 1$ h) and sustained the release of insulin over 3 days, whereas plain insulin was not detected after 24 h. The main pharmacokinetic parameters obtained from both, microemulsions and insulin solutions have been summarized in Table 2. Area under the curve (AUC) for microemulsions showed almost a 10-fold increment from AUC generated after administering plain insulin solution indicating a significant enhancement of insulin's bioavailability when given orally as microemulsions. AUCs were generated using standard trapezoidal rule applicable for pharmacokinetics of oral formulations. The enhanced absorption may be explained in terms of (a) huge specific surface area of the microemulsion droplets, (b) altered permeability of the intestinal mucosa because of DMAB which promotes improved permeation of insulin across the gastric barrier, (c) reduction in the interfacial tension between the formulation and lipophilic mucosal layers and (d) due to enhanced stability of insulin inside the core of microemulsion against gastric proteases and acidic microenvironment. Furthermore, the other components of the microemulsion formulations (TA and PG) are expected to promote permeation due to their interaction with intestinal lipids making them suitable excipients for such formulations [35]. On the other hand, the microemulsion uptake by most widely accepted path, the M cells of the Peyer's patches in the intestinal region cannot be overruled. Moreover, the aqueous milieu inside the core of microemulsions provide an ambient environment free from changes in pH and ionic conditions, which further protects the insulin and accounts for its stability inside the core. In fact, a small amount of insulin after oral solution administration was detected in the blood by ELISA indicating that it was directly absorbed, and this direct uptake of insulin has been

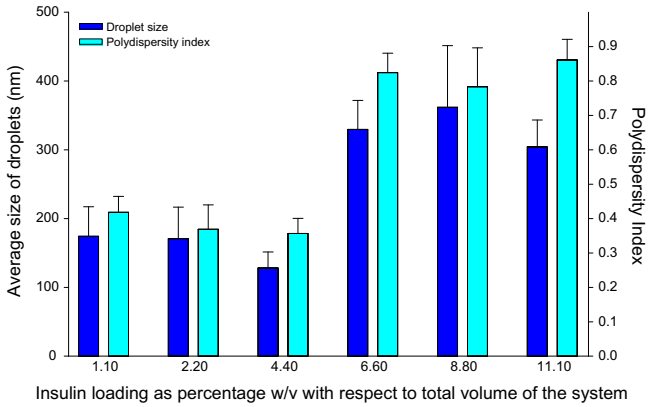

Fig. 9. Effect of insulin loading in the aqueous phase on size and PDI of microemulsion droplets at 25 °C. The original formulations had 2.2% w/v as insulin loading in 0.05 M sodium hydroxide making 20% aqueous phase. Data represents mean with standard deviation at $n = 3$. (For interpretation of the references to colour in this figure legend, the reader is referred to the web version of this article.)

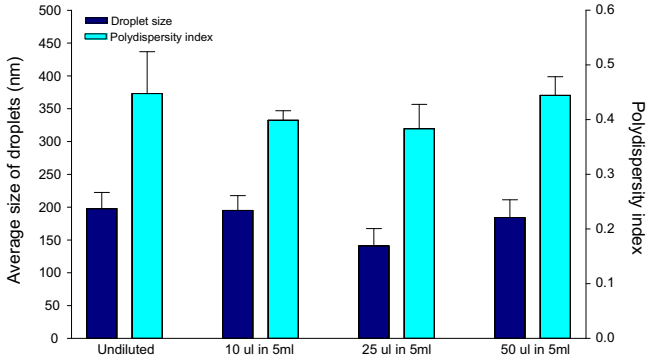

Fig. 10. Effect of dilution of microemulsion with water on droplet size and PDI of microemulsion droplets at 25 °C. The original formulations had 2.2% w/v as insulin loading in 0.05 M sodium hydroxide making 20% aqueous phase. Data represents mean with standard deviation at $n = 3$. (For interpretation of the references to colour in this figure legend, the reader is referred to the web version of this article.)

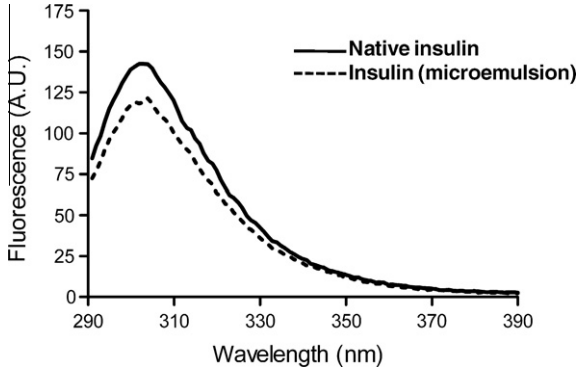

Fig. 11. Intrinsic fluorescence emission spectra of native bovine insulin (solid line) and bovine insulin extracted from the nano-droplets (dotted line). The solutions were excited at 280 nm, and emission was monitored from 290 to 300 nm. Excitation and emission slits widths were 5 nm each. Each spectrum is the mean of three scans at 25 °C.

attributed to specific insulin receptors in intestinal enterocytes and rapid internalization by the epithelial cells to the interstitial space from which it reached the blood circulation [36]. Tissue distribution analysis revealed significant levels of insulin in various tissues over 72 h in microemulsion group, whereas group administered

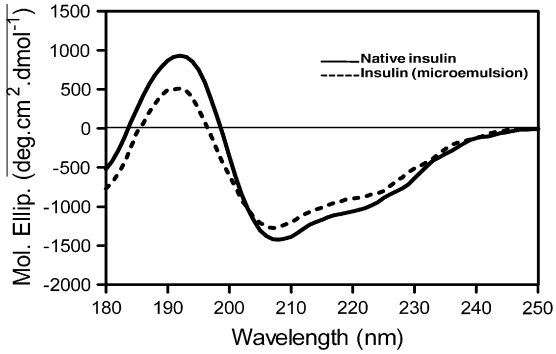

Fig. 12. Circular dichroism spectra of native bovine insulin solution (solid line) and bovine insulin extracted from the nano-droplets (dotted line) in the far UV region. The concentration of insulin used was 100 μg/ml for the native solution, and the extracted insulin was diluted to the same amount. The path length was 0.01 cm, and the data shows the mean of three scans at 25 °C.

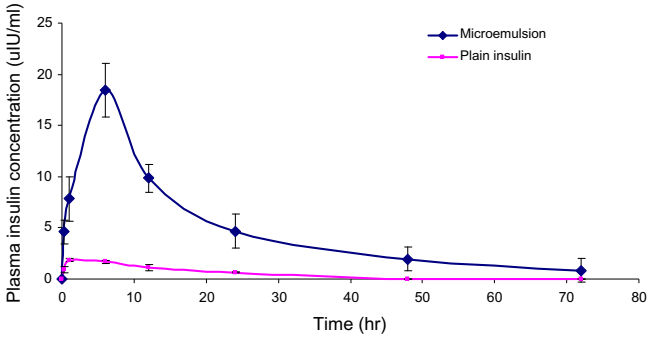

Fig. 13. Comparative *in vivo* profiles of insulin loaded microemulsions and plain insulin solution in phosphate buffer saline, administered orally at a dose of 20 IU/kg. Blood levels of insulin were determined using bovine insulin specific ELISA kits. Microemulsions sustained the release of insulin till 3 days, whereas insulin from plain solution was not detected after 24 h. Each data point represents mean with standard deviation at $n = 3$. (For interpretation of the references to colour in this figure legend, the reader is referred to the web version of this article.)

with plain insulin solution had very low levels of insulin which were not detected after 24 h (Fig. 14). It appears that microemulsion had longer residence time in the body compared to the plain insulin solution that was cleared rapidly, and no more insulin was detected from this group, which demonstrated altered pharmacokinetic profile of orally administered insulin when given as microemulsion when compared to rats orally administered with plain insulin solution. Microemulsions offered distinct advantage over plain insulin when given orally because of their fine particle size (in nm range) that prevented their rapid clearance from systemic circulation, and additionally the surfactant (DMAB) and oil phase (TA) coating on microemulsions protected the aqueous core of microemulsions against proteolytic enzymes in the blood. Moreover, the enhanced systemic absorption of insulin from orally administered microemulsions can be attributed to the increased solubility of insulin at a pH between 5 and 7 normally at which insulin is insoluble and precipitates out of solution. The altered tissue distribution of insulin from microemulsion formulations resulted in increased sequestration of insulin in tissues including the spleen, pancreas, heart, liver, brain, lungs and kidney (till 72 h compared with 24 h from plain insulin solution), which has well known physiological significance with respect to normal insulin function in different tissues as insulin is required in spleen for lipogenesis, it modulates the pancreatic juice with respect to amylase, lipase and trypsin content, prevents cardiomyopathy in cardiac tissues. In liver, insulin stimulates glycogenesis by

Table 2
Pharmacokinetic parameters of insulin after oral administration of pure drug solution and microemulsion formulations.

Formulations	C_{max} (μIU/ml)	T_{max} (h)	AUC_{0-t} (μIU/ml h)	$T_{1/2}$ a (h)	$T_{1/2}$ e (h)	Cl (ml/h)	Vd (ml)
Plain insulin solution	1.84 ± 0.1	1 ± 0.0	36.7	0.084	15.72	0.646	14.66
Microemulsion*	18.4 ± 2.6	6 ± 0.0	356.1	0.483	20.08	0.151	4.38

Data presented as mean ± standard deviation ($n = 3$).
C_{max}: maximum plasma concentration, T_{max}: time taken to attain C_{max}, AUC: areas under the plasma concentration–time curve; AUCs were calculated using the standard trapezoidal rule.
$p < 0.05$ versus plain insulin solution.
$T_{1/2}$ a: T half absorption.
$T_{1/2}$ e: T half elimination.
Cl: clearance.
Vd: volume of distribution.

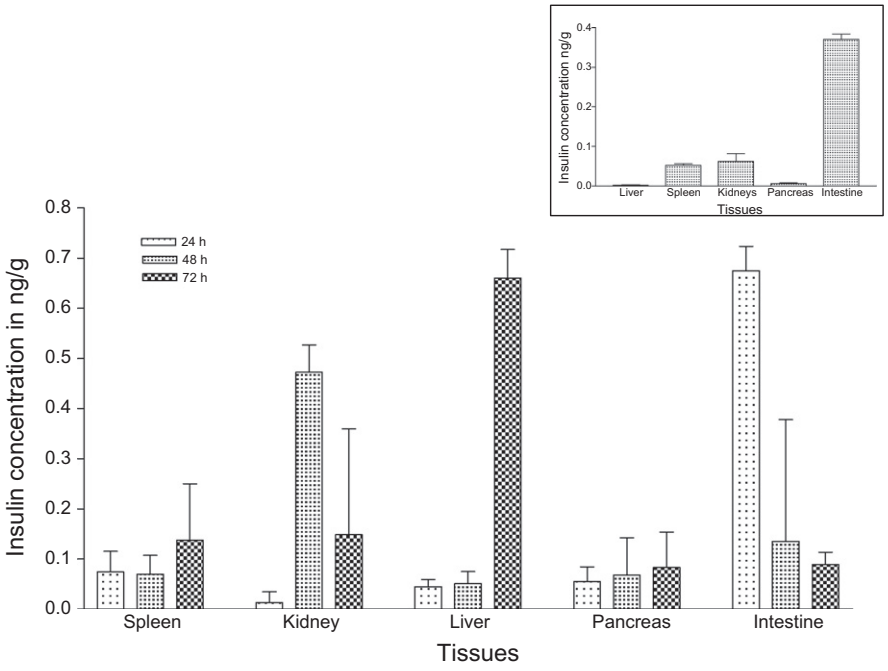

Fig. 14. Tissue distribution profiles of insulin loaded microemulsions (over 72 h) and plain insulin solution over 24 h (inset) in phosphate buffer saline, administered orally at a dose of 20 IU/kg. Blood levels of insulin were determined using bovine insulin specific ELISA kits. Microemulsions sustained the release of insulin till 3 days, whereas insulin from plain solution was not detected after 24 h. Each data point represents mean with standard deviation at $n = 3$.

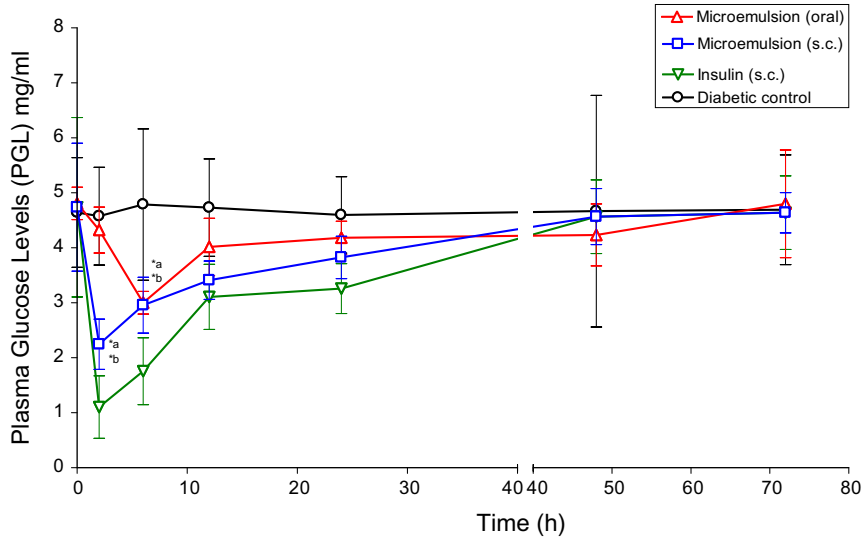

Fig. 15. Plasma glucose levels (PGL) obtained after oral (triangles) and subcutaneous (squares) administration of insulin loaded microemulsions in streptozotocin induced diabetic animals compared with PGL obtained using subcutaneous administration of insulin solution (in phosphate buffer saline) at a dose of 20 IU/kg body weight of the animals. Values reported are mean ± SEM ($n = 6$). Significant differences of the mean values were evaluated by Student's t-test. A p-value of <0.05 was considered significant: (a) versus insulin solution (s.c.); (b) versus untreated group. (For interpretation of the references to colour in this figure legend, the reader is referred to the web version of this article.)

promoting the enzyme glycogen synthase which is responsible for conversion of glucose to glycogen. In brain, insulin increases glucose uptake in cortical areas, promotes memory and learning, prevents dementia and is required for normal synaptic functioning and brain plasticity. In lungs, insulin regulates energy homeostasis and inflammation by modulating levels of PPAR-α and PPAR-δ, whereas in kidneys insulin is required physiologically for the proliferation of renal cells and stimulates the production of other important growth factors such as insulin-like growth factor-1 and transforming growth factor-β.

3.8. Pharmacodynamic studies in streptozotocin induced diabetes model

Fig. 15 shows PGL obtained in STZ induced diabetic rats after administration of insulin loaded microemulsion via oral and subcutaneous route and plain insulin solution administered via subcutaneous route at a dose of 20 IU/kg. In group I (positive control), no significant change in PGL was observed till the studied period (72 h) except for few insignificant fluctuations. Group II administered orally with insulin loaded microemulsion displayed PGL around 3.0 mg/ml at 6 h, which corresponded to 37.5% reduction in PGL (value compared with PGL before the treatment at 0 time point), and it returned to hyperglycaemic levels by 72 h, whereas in group treated subcutaneously with insulin loaded microemulsions (group III), PGL was decreased to 2.24 mg/ml by 2 h (corresponding to 52.3% reduction in PGL compared with PGL values before the treatment), and it returned to hyperglycaemic levels by 48 h. This demonstrated the potential of insulin loaded microemulsions in controlling hyperglycaemia via oral and subcutaneous route. Group administered with plain insulin solution subcutaneously showed the maximum reduction in PGL (~1.1 mg/ml corresponding to 76.59% reduction in PGL compared with PGL values before the treatment) by 2 h and hyperglycaemic levels were returned by 48 h. All the glucose reduction values in formulation treated rats were biologically and statistically significant and represented the ability of these colloidal carriers in controlling hyperglycaemia and releasing insulin *in vivo* when administered via oral and subcutaneous route. Combined with pharmacokinetic results where microemulsions displayed longer $T_{1/2}$ elimination of 20 h (compared to ~15 h with plain insulin solution) and reduced clearance (0.151 from microemulsion compared to 0.646 ml/h from plain insulin solution), a significant alteration in pharmacokinetic profile of insulin was observed which in fact was also reflected in the streptozotocin induced diabetic study where microemulsions displayed glucose-lowering potential via both oral and subcutaneous routes. Insulin loaded microemulsions (via subcutaneous and oral route) displayed a sustained hypoglycaemic activity illustrating the pharmacodynamic efficacy of the formulations with maximum reduction in PGL (37.5%) at 6 h at 20 IU/kg dose of insulin.

4. Conclusions

Microemulsions encapsulating insulin can be made by a reverse micellar approach under low shear process conditions that are able to preserve the secondary structure of insulin in the short term. This preliminary data clearly indicates the ability of microemulsions to improve the oral bioavailability of insulin with modest effects on blood glucose levels in diabetic rats. Moreover, an oral formulation like this would certainly improve patient compliance and adherence to the insulin therapy because of its non-invasive and painless nature compared to insulin injections. Further studies are required to examine the potential of reverse micellar systems for efficient management of hyperglycaemia.

Acknowledgements

K.W. was supported by an EPSRC MRes studentship and G.S. by a University of Strathclyde Ph.D. studentship. Start-up funds from University of Strathclyde to M.N.V.R.K. are gratefully acknowledged, along with instrument support from the EPSRC, Grant Ref. EP/E036244/1.

References

[1] F.G. Banting, C.H. Best, J.B. Collip, W.R. Campbell, A.A. Fletcher, Pancreatic extracts in the treatment of diabetes mellitus, Preliminary report, Can. Med. Assoc. J. 12 (1922) 141–146.
[2] R. Hanas, J. Ludvigsson, Experience of pain from insulin injections and needle-phobia in young patients with IDDM, Pract. Diabetes Int. 14 (2005) 95–99.
[3] O. Pillai, R. Panchagnula, Insulin therapies-past, present and future, Drug Discov. Today 6 (2001) 1056–1061.
[4] J.P. Bai, L.L. Chang, Transepithelial transport of insulin. I. Insulin degradation by insulin degrading enzyme in small intestinal epithelium, Pharm. Res. 12 (1995) 1171–1175.
[5] W.C. Duckworth, R.G. Bennett, F.G. Hamel, Insulin degradation: progress and potential, Endocr. Rev. 19 (1998) 608–624.
[6] E. Wajcberg, Y. Miyazaki, C. Triplitt, E. Cersosimo, R.A. Defronzo, Dose–response effect of a single administration of oral hexyl-insulin monoconjugate 2 in healthy nondiabetic subjects, Diabetes Care 27 (2004) 2868–2873.
[7] A. Yamamoto, T. Taniguchi, K. Rikyuu, et al., Effects of various protease inhibitors on the intestinal absorption and degradation of insulin in rats, Pharm. Res. 11 (1994) 1496–1500.
[8] Z. Shao, Y. Li, T. Chermak, A.K. Mitra, Cyclodextrins as mucosal absorption promoters of insulin. II. Effects of beta-cyclodextrin derivatives on alpha-chymotryptic degradation and enteral absorption of insulin in rats, Pharm. Res. 11 (1994) 1174–1179.
[9] S. Eaimtrakarn, Y.V. Rama Prasad, T. Ohno, et al., Absorption enhancing effect of labrasol on the intestinal absorption of insulin in rats, J. Drug Target. 10 (2002) 255–260.
[10] N. Kahyap, N. Kumar, M.N.V.R. Kumar, Hydrogels for pharmaceutical and biomedical applications, Crit. Rev. Ther. Drug Carrier Syst. 22 (2005) 107–150.
[11] R.S. Spangler, Insulin administration via liposomes, Diabetes Care 13 (1990) 911–922.
[12] H.A. Krauland, D. Guggi, A. Bernkop-Schnurch, Thiolated chitosan microparticles: a vehicle for nasal peptide drug delivery, Int. J. Pharm. 307 (2006) 270–277.
[13] C. Damge, C. Michel, M. Aprahamian, P. Couvrerur, New approach for oral administration of insulin with polyalkylcyanoacrylate nanocapsules as drug carrier, Diabetes 37 (1998) 246–251.
[14] A. Çilek, N. Çelebi, F. Tırnaksız, A. Tay, Lecithin-based microemulsions of rh-insulin with aprotinin for oral administration: investigation of hypoglycemic effects in non-diabetic and STZ-induced diabetic rats, Int. J. Pharm. 298 (2005) 176–185.
[15] M.J. Schick, in: P.L. Luisi, B.E. Straub (Eds.), Reverse Micelles, Plenum, New York, 1984, p. 354.
[16] S.F. Matzke, A.L. Creagh, C.A. Haynes, J.M. Prausnitz, H.W. Blanch, Mechanisms of protein solubilization in reverse micelles, Biotech. Bioeng. 40 (1992) 91–102.
[17] Y. Liu, X. Dong, Y. Sun, New development of reverse micelles and applications in protein separation and refolding, Chin. J. Chem. Eng. 16 (2008) 949–955.
[18] M.P. Pileni, Reverse micelles as microreactors, J. Phys. Chem. 97 (1993) 6961–6973.
[19] M.J. Lawrence, G.D. Rees, Microemulsions-based media as novel drug delivery systems, Adv. Drug Deliv. Rev. 45 (2000) 89–121.
[20] C.C. Müller-Goymann, Physicochemical characterization of colloidal drug delivery systems such as reverse micelles, vesicles, liquid crystals and nanoparticles for topical administration, Eur. J. Pharm. Biopharm. 58 (2004) 343–356.
[21] V. Bhardwaj, S. Hariharan, I. Bala, A. Lamprecht, N. Kumar, R. Panchagnula, M.N.V.R. Kumar, Pharmaceutical aspects of polymeric nanoparticles for oral delivery, J. Biomed. Nanotech. 1 (2005) 235–258.
[22] S. Watnasirichaikul, N.M. Davies, T. Rades, I.G. Tucker, Preparation of biodegradable insulin nanocapsules from biocompatible microemulsions, Pharm. Res. 17 (2000) 684–689.
[23] I. Danielsson, B. Lindman, The definition of a microemulsion, Colloids Surf. 3 (1981) 391–392.
[24] Z.E. Proverbio, S.M. Bardavid, E.L. Arancibia, P.C. Schulz, Hydrophile–lipophile balance and solubility parameter of cationic surfactants, Colloids Surf. 214 (2003) 167–171.
[25] V. Bhardwaj, D.D. Ankola, S.C. Gupta, M. Schneider, C.M. Lehr, M.N.V.R. Kumar, PLGA nanoparticles stabilized with cationic surfactant: safety studies and application in oral delivery of paclitaxel to treat chemical induced breast cancer in rat, Pharm. Res. 26 (2009) 2495–2503.
[26] M.Z. Fiume, Final report on safety assessment of Triacetin, Int. J. Toxicol. 22 (2003) 1–10.
[27] C. Solans, P. Izquierdo, J. Nolla, N. Azemar, M.J. Garcia, Nano-emulsions, Curr. Opin. Colloid Interface Sci. 10 (2005) 102–110.

[28] J. Liu, T. Gong, C. Wang, Z. Zhong, Z. Zhang, Solid lipid nanoparticles loaded with insulin by sodium cholate-phosphatidylcholine-based mixed micelles: preparation and characterization, Int. J. Pharm. 340 (2007) 153–162.
[29] P. Fernandez, V. Andre, J. Reiger, A. Kuhnle, Nano-emulsion formation by inversion phase inversion, Colloids Surf. A Physiochem. Eng. Aspects 251 (2004) 53–58.
[30] W.S. Annan, M. Fairhead, P. Pereria, C.F. van der Walle, Emulsifying performance of modular β-sandwich proteins: the hydrophobic moment and conformational stability, Protein Eng. Des. Sel. 19 (2006) 537–545.
[31] A. Forgiarini, J. Esquena, C. González, C. Solans, Formation of nano-emulsions by low-energy emulsification methods at constant temperature, Langmuir 17 (2001) 2076–2083.
[32] P.S. Pourhosseini, A.A. Saboury, F. Najafi, M.N. Sarbolouki, Interaction of insulin with a triblock copolymer of PEG-(fumaric-sebacic acids)-PEG: thermodynamic and spectroscopic studies, Biochim. Biophys. Acta 1774 (2007) 1274–1280.
[33] E. Gok, S. Ates, Fluorimetric detection of insulin in the presence of Eu(III) – {pyridine-2,6-dicarboxylate} tris complex, Turk. J. Chem. 25 (2001) 81–91.
[34] M.J. Ettinger, S.N. Timasheff, Optical activity of insulin, I. On the nature of the circular dichroism bands, Biochemistry 10 (1971) 824–840.
[35] C.J.H. Porter, C.W. Pouton, J.F. Cuine, W.N. Charman, Enhancing intestinal drug solubilisation using lipid-based delivery systems, Adv. Drug Deliv. Rev. 60 (2008) 673–691.
[36] M. Bendayan, E. Ziv, D. Gingras, R. Ben-Sasson, H. Bar-On, M. Kidron, Biochemical and morpho-cytochemical evidence for the intestinal absorption of insulin in control and diabetic rats. Comparison between the effectiveness of duodenal and colon mucosa, Diabetologia 37 (1994) 119–126.